REAL-TIME LEADER-FOLLOWER UAV FORMATION FLIGHT BASED ON MODIFIED NONLINEAR GUIDANCE

Chulwoo Park*, Hyoun Jin Kim*, Youdan Kim*
*Seoul National University, South Korea

Keywords: *Multiple UAV, Modified Nonlinear Guidance, Information Synchronization*

Abstract

To perform formation flight of multiple UAVs (Unmanned Aerial Vehicles), an accurate guidance law is required. Existing guidance law based on nonlinear path-following guidance method provides outstanding path following performance. However, the nonlinear guidance law does not reflect the characteristics of UAV, and therefore the performance of the guidance law may be degraded in the real environment. In this study, model-based modified nonlinear guidance law is proposed so that a lateral acceleration command generated by the proposed guidance law coincides with actual lateral acceleration of the UAV. Utilizing the proposed nonlinear guidance law, leader-follower formation flight controller is designed. Multi-UAV simulation based on the identified linear model of UAV is performed to demonstrate the performance of the proposed method. Hardware system of multiple UAVs is constructed, and flight test is conducted to validate the proposed algorithm.

1 Introduction

Autonomous formation flight of UAVs is required to perform various cooperative missions using multiple UAVs. Especially, for formation flight, a precise guidance law is needed. There have been lots of studies on the formation flight of multiple UAVs [1-4]. Nonlinear path-following guidance law [1] and NLDI (Nonlinear Dynamic Inversion) guidance law [2] were introduced for the formation flight of two UAVs. In [3], autonomous formation experiment of two fixed-wing UAVs was conducted based on hybrid method. In [4],

controller of three rotary-wing UAVs was designed for cooperative payload transportation. For formation flight, precise guidance law should be designed especially in lateral axis rather than longitudinal axis. Usually, fixed-wing UAV lateral guidance is related with a turning motion by roll command. Guidance law generates a lateral command with an assumption that the fixed-wing UAV performs a coordinated turn during the turn maneuver. However, 6-DOF(Degree Of Freedom) numerical simulation and/or flight tests show that UAV does not perform exact coordinated turn because of the aerodynamic effects of control surfaces and trim condition. This may degrade the performance of the guidance law especially for high aspect ratio or rudderless aircraft that adverse yaw effect appears considerably. In this study, a nonlinear guidance law is proposed to deal with this problem, which can be used for real-time UAV formation flight. This paper is organized as follows. In section II, system model and identification process of target UAV are introduced. In section III, modified nonlinear lateral guidance is proposed. Also, lateral acceleration is estimated by comparing lateral acceleration by the guidance command and actual centripetal acceleration for the flight condition of steady-state loitering which is used to modify the guidance command. 6-DOF numerical linear simulation is performed to demonstrate the performance of the proposed guidance law. In section IV, formation flight test result in shown, and finally, conclusion is made in section V.

2 Design and Modeling of Multi-UAV System

In this study, off the shelf RC(Radio Control) airplane and customized 3D printed canopy are

considered for UAV system. For autonomous formation flight, each UAV should share its own information with other UAVs, and synchronization of multi-UAV is performed by a cyclic communication manner. For the model-based guidance law, a mathematical model is needed, and the linear system identification of UAV is carried out.

2.1 Airframe of Multiple UAV

To select the airframe of UAV, robustness and portability are mainly considered due to frequent take-off and landing of more than three UAVs. A wooden airframe is not suitable for this situation. Instead, an EPO(Expanded Ploy Ethylene)/EPP(Expanded Poly Propylene) airframe is proper because of its durable and detachable characteristics. For the attitude control of the UAV, the UAV should have AOA (Angle of Attack), AOS(Angle of Sideslip), and pitot-static sensors, and therefore pusher-type airplane is preferred. For these reasons, an RC airplane (Hitec Skyscout) shown in Fig. 1 has been selected for this study, which is made up of durable EPO material and has a pusher-type configuration with folding prop.

Fig. 1 Target Radio-controlled (RC) airplane

2.2 Flight Control Computer and Avionics

All the onboard sensors, RC receiver and actuators are connected to the FCC (Flight Control Computer) with ARM Cortex-M3. Microstrain 3DM-45 AHRS (Attitude Heading Reference System) sensor is chosen to provide the information of attitude, velocity and position at 50Hz. Relative air speed is measured by using pitot-static tube, and AOA/AOS sensors provide

angle of attack and side slip angle information. Onboard MS-5611 absolute pressure sensor provides pressure altitude. For multiple UAV communication, 900MHz Xbee-Pro module is used for telemetry.

2.3 Linear System Identification

The flight for system identification has been performed to determine lateral and longitudinal linear system models [5]. Multistep 3-2-1-1 inputs are used for the control inputs of aileron, elevator, and rudder, while doublet input is used for the control input of throttle. Lateral system identification flight and longitudinal system identification flight are performed separately. State variables and control inputs are recorded at 50Hz by ground control system through RF telemetry. System matrix parameters are estimated by MATLAB System Identification Toolbox™. The lateral and longitudinal linear models are estimated as follows

$$
\begin{bmatrix} \dot{\beta} \\ \dot{\phi} \\ \dot{p} \\ \dot{r} \end{bmatrix} = \begin{bmatrix} 0 & 0.7231 & -0.1718 & -1.6319 \\ 0 & 0 & 0.9957 & -0.0942 \\ -53.0053 & 0 & -10.5207 & 10.4250 \\ 7.3627 & 0 & -3.3925 & -4.8898 \end{bmatrix} \begin{bmatrix} \beta \\ \phi \\ p \\ r \end{bmatrix}
$$
$$
+ \begin{bmatrix} -1.4129 & -1.7054 \\ 0 & 0 \\ -51.1925 & 8.2723 \\ -9.0546 & -13.6097 \end{bmatrix} \begin{bmatrix} \delta_{ail} \\ \delta_{rud} \end{bmatrix} \quad (1)
$$

$$
\begin{bmatrix} \dot{V} \\ \dot{\alpha} \\ \dot{\theta} \\ \dot{q} \end{bmatrix} = \begin{bmatrix} 0 & 25.0414 & -9.7545 & 0 \\ -0.4130 & -12.0086 & 0.9435 & 2.2203 \\ 0 & 0 & 0 & 1 \\ -0.1204 & -23.5155 & 0 & -0.6636 \end{bmatrix} \begin{bmatrix} V \\ \alpha \\ \theta \\ q \end{bmatrix}
$$
$$
+ \begin{bmatrix} 0.0080 & 10.0711 \\ 0.0003 & 3.2113 \\ 0 & 0 \\ -0.0039 & -15.3344 \end{bmatrix} \begin{bmatrix} \delta_{thr} \\ \delta_{ele} \end{bmatrix} \quad (2)
$$

The above system dynamic model represents the target RC airplane in a steady level flight at 13m/s and 70m of altitude. To verify the estimated lateral/longitudinal linear model, simulation result using the identified linear model is compared with actual flight data for the same control input condition. Figures 2 and 3 show the simulation results using the identified model and actual flight data, and it

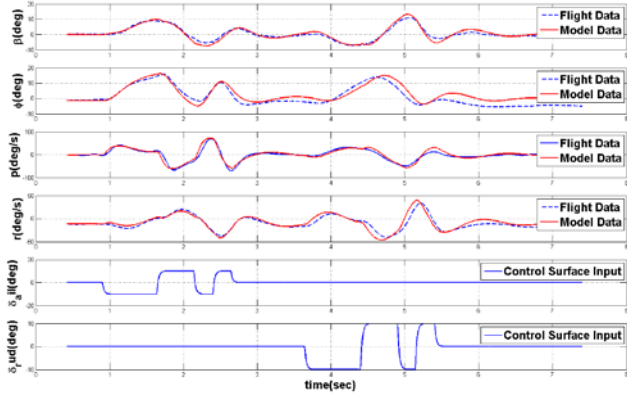can be concluded that the identification is performed successfully.

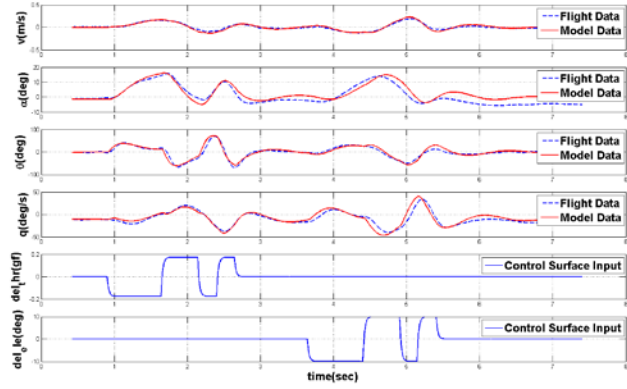**Fig. 2** Comparison of Actual Flight Data versus Identified Model (Lateral)

Fig. 3 Comparison of Actual Flight Data versus Identified Model (Longitudinal)

3 Modified Nonlinear Guidance

Usually, lateral guidance command causes a great influence on the formation flight of UAVs, which yields turning motion of UAV. In model independent guidance algorithms [1], it is assumed that UAV always performs coordinated turn, which is not true in real flight because of the aerodynamic effects of control surfaces and trim condition of the UAV. This may degrade the performance of the guidance law and cause large path following error. In this section, the lateral guidance acceleration error is analyzed to modify the guidance command. Model-based analysis is performed to provide modification function.

3.1 Lateral Acceleration Command

The nonlinear guidance law in [1] has been originated from a proportional navigation (PN) guidance law [6]. Figure 4 shows a geometry of the nonlinear lateral guidance law. In Fig. 4, L is a distance between UAV and a virtual moving target point on desired flight path.
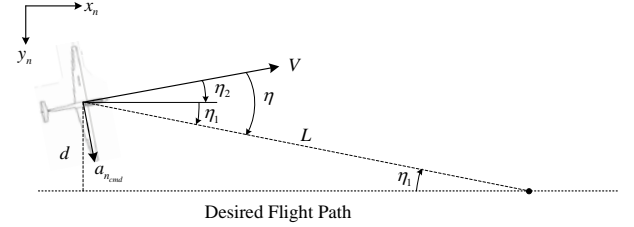

Fig. 4 Geometry of Nonlinear Guidance Law

In the lateral guidance law, by using a geometrical relationship of a velocity vector and a desired flight path, a lateral acceleration command $a_{n_{cmd}}$ can be calculated as follows.

$$a_{n_{cmd}} = \frac{2V^2}{L}\sin\eta \qquad (3)$$

To make the UAV follow the acceleration command $a_{n_{cmd}}$, a roll command ϕ_{cmd} can be used assuming that the UAV performs a coordinated turn with a centripetal acceleration a_{cen}.

$$\phi_{cmd} = \tan^{-1}\left(\frac{a_{n_{cmd}}}{g}\right) \quad where \ \ a_{n_{cmd}} = a_{cen} \qquad (4)$$
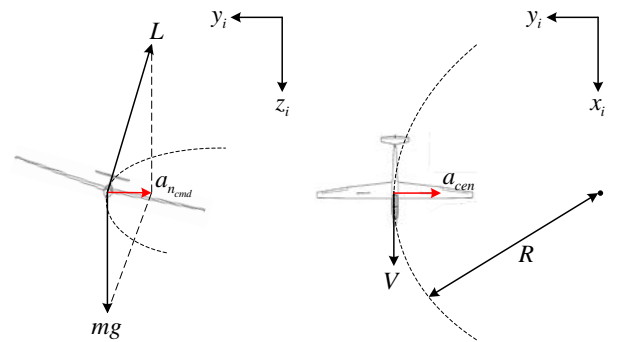

Fig. 5 Normal Acceleration and Centripetal Acceleration

However, the acceleration $a_{n_{cmd}}$ generated by roll command ϕ_{cmd} does not match with the actual acceleration a_{cen}, because the UAV does not perform a coordinated turn when the roll angle is changed due to the adverse yaw effect.

To perform accurate lateral maneuver, $a_{n_{cmd}}$ by the nonlinear guidance should be modified to coincide with a_{cen}. To do this, a function $f(\cdot)$ of the acceleration relation between $a_{n_{cmd}}$ and a_{cen} is first obtained using the simulation data with the identified model. The function $f(\cdot)$ represents the actual characteristic of the UAV.

$$a_{cen} = f(a_{n_{cmd}}) \qquad (5)$$

With the function $f(\cdot)$, the modification function $g(\cdot)$ can be obtained to modify $a_{n_{cmd}}$ as

$$a_{n_{cmd_{mod}}} = g(a_{n_{cmd}}) \qquad (6)$$

Note that the function $g(\cdot)$ is an inverse function of $f(\cdot)$ for one-to-one matching of acceleration as follows

$$g(\cdot) = f^{-1}(\cdot) \qquad (7)$$

Therefore, the modification function $g(\cdot)$ makes a_{cen} match with $a_{n_{cmd}}$.

$$a_{cen} = f(a_{n_{cmd_{mod}}})$$
$$a_{cen} = f(g(a_{n_{cmd}})) = f(f^{-1}(a_{n_{cmd}})) \qquad (8)$$
$$a_{cen} = a_{n_{cmd}}$$

In this study, the acceleration relationship function $f(\cdot)$ is modeled as a linear function, which is estimated by least square method. Therefore, the modification function $g(\cdot)$ is also a linear function.

3.2 Acceleration Relationship Function

To formulate the modification function $g(\cdot)$, the acceleration relationship function $f(\cdot)$ should be obtained first.

$$a_{cen} = f(a_{n_{cmd}}) = C_1 a_{n_{cmd}} + C_2 \qquad (9)$$

The relationship between the lateral acceleration command $a_{n_{cmd}}$ and the centripetal acceleration a_{cen} can be identified by using simulation result for steady state loitering flight condition. The steady state loitering flight condition generates a constant lateral acceleration command, and therefore it is a proper maneuver for observing the relation of accelerations. For the specified lateral acceleration value $a_{n_{cmd}}$, the resultant centripetal acceleration a_{cen} is calculated by using the following relation of average turning radius R_{avr} and cruising velocity V_{avr}.

$$a_{cen} = \frac{V_{avr}^2}{R_{avr}} \qquad (10)$$

For various $a_{n_{cmd}}$ values, 6-DOF linear simulation result of the target UAV loitering flight is shown in Fig. 6. The longitudinal command maintains a level flight, while the lateral command makes the UAV follow the roll command ϕ_{cmd}.
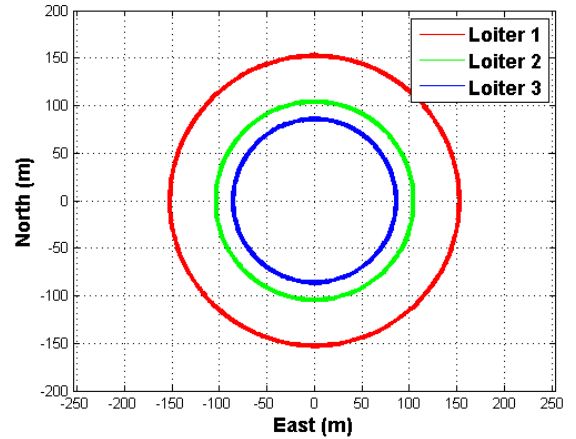

Fig. 6 Simulation Result of Loitering Flight

Table 1 Acceleration Result of Simulation

	$a_{n_{cmd}}$	a_{cen}	R_{avr}	V_{avr}
Loiter 1	1.452	1.107	152.7	13.0
Loiter 2	2.142	1.616	104.6.	13.0
Loiter 3	2.626	1.968	85.9	13.0

Table 1 summarizes the result of the acceleration relation by numerical simulation.

Using these data, the function $f(\cdot)$ can be estimated by the least square method as follows

$$f(a_n) = C_1 a_n + C_2 = 0.753 a_n + 0.000 \qquad (11)$$

The coefficient C_1 of $f(\cdot)$ is 0.753, which means that $a_{n_{cmd}}$ does not agree with a_{cen}, i.e., the generated acceleration is not sufficient. Note that the coefficient C_2 of $f(\cdot)$ is zero because the linear model has a symmetrical structure. Figure 7 shows the result of $f(\cdot)$.
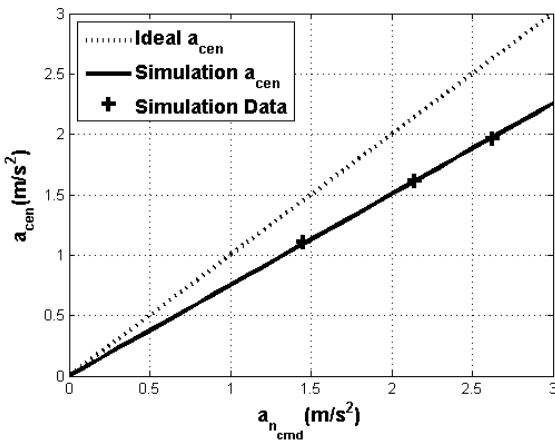

Fig. 7 $f(\cdot)$ via Simulation

3.3 Acceleration Modification Function

As shown in Fig.7, the lateral acceleration command $a_{n_{cmd}}$ is not sufficient to generate the corresponding centripetal acceleration a_{cen}. This mismatch degrades the guidance performance, and therefore $a_{n_{cmd}}$ should be modified. As shown un Eq. (7), $g(\cdot)$ is an inverse function of $f(\cdot)$, and it can be simply calculated as follows

$$g(a_n) = f^{-1}(a_n) = \frac{1}{C_1} a_n - \frac{C_2}{C_1} \qquad (12)$$

The lateral acceleration command $a_{n_{cmd}}$ generated by the nonlinear guidance is an input of the modification function $g(\cdot)$. Therefore, the actual acceleration command is changed as follows

$$g(a_n) = 1.328 a_n + 0.000 \qquad (13)$$

Now, numerical simulation for square path following is performed using the modified nonlinear guidance law with Eq. (13). Figure 8 shows the path tracking simulation result using the original nonlinear guidance law compared with that using the modified nonlinear guidance law. The guidance command is changed in each corner of the square path, and this change generates displacement error periodically. The modified guidance command improves the performance of the path following as shown in Fig. 8. The average displacement error is 4.81m without considering $g(\cdot)$, but the error reduces to 3.15m by the modification. The error is reduced 34.5% at this particular case of the square path tracking. The peak path error and the average displacement error are summarized in Table 2.
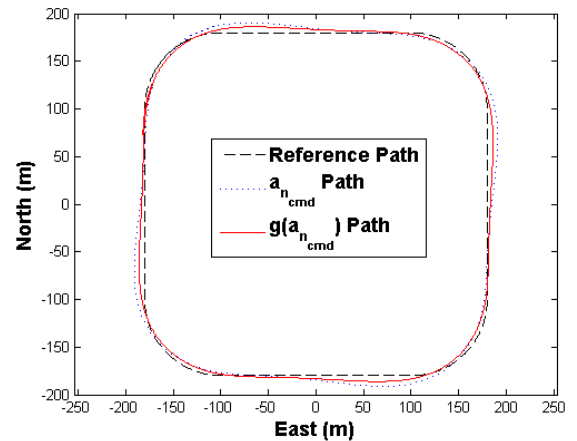

Fig. 8 Path Comparison of Modified Guidance

Table 2 Path Following Comparison Result

	$a_{n_{cmd}}$	$g(a_{n_{cmd}})$	Reduction
Peak Path Error(m)	11.26	6.22	44.8%
Average Path Error(m)	4.81	3.15	34.5%

4 Modified Guidance Flight Test

In this section, the performance of the proposed acceleration modification method is demonstrated by flight test. The functions $f(\cdot)$ and $g(\cdot)$ are re-calculated by using the steady-state loitering flight test data. Finally, the modified nonlinear guidance law is applied for the flight test. Using the modified nonlinear guidance law, leader-follower flight test of two UAVs are also conducted.

4.1 Algorithm Verification Flight Test

To verify the proposed acceleration modification algorithm, loitering flight test is conducted. The condition of the flight is steady-state loitering and level flight at 60m altitude. Loitering of UAV is performed by tracking a predefined circular path using the nonlinear path following guidance. In the modified nonlinear guidance law, only the changed roll angle and geometrical circle radius are used to calculate the acceleration. Three loitering flight results are shown in Fig.9. By using the flight test data, the acceleration relationship function $f(\cdot)$ is estimated again. Table 3 summarizes the obtained result of the acceleration relation by the flight test.

Table 3 Acceleration Result of Flight Test

	$a_{n_{cmd}}$	a_{cen}	R_{avr}	V_{avr}
Loiter 1	1.196	0.945	152.4	12.0
Loiter 2	1.558	1.246	100.7	11.2
Loiter 3	1.828	1.472	82.3	11.0

Fig. 9 Result of Loitering Flight

The acceleration function $f(\cdot)$ is estimated by using the flight test data as

$$f(a_n) = 0.801a_n - 0.002 \qquad (14)$$

Figure 10 shows the result. The estimated function of Eq. (14) is a little bit different from the function of Eq. (11). Now, the modification function $g(\cdot)$ is calculated using Eq. (14) as

$$g(a_n) = 1.249a_n - 0.002 \qquad (15)$$

The calculated $g(\cdot)$ is used to modify the lateral nonlinear guidance command. Flight tests are conducted to verify the modification. The flight result using the modified guidance command is shown in Fig. 11.
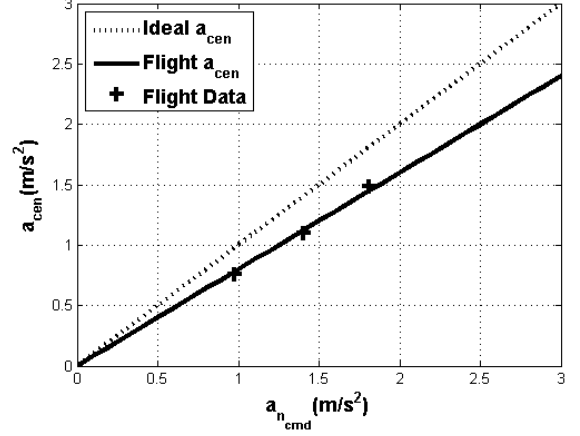

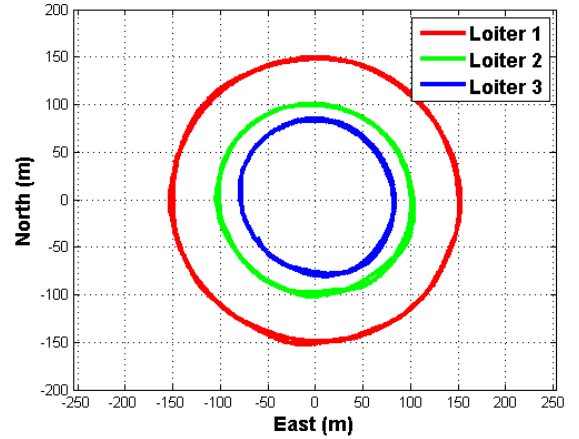**Fig. 10** $f(\cdot)$ via Flight Test

Fig. 11 Result of Modified Loitering Flight

After modified loitering flight, the acceleration relation function $f(\cdot)$ is re-estimated. Table 4 summarizes the obtained result of the acceleration relation by the modified flight test.

$$f(a_n) = 0.936a_n + 0.019 \qquad (16)$$

Table 4 Acceleration Result of Modified Flight

	$a_{n_{cmd}}$	a_{cen}	R_{avr}	V_{avr}
Loiter 1	0.800	0.811	149.3	11.0
Loiter 2	1.449	1.376	98.8	11.7
Loiter 3	1.526	1.438	77.7	10.6

Because the loitering command is generated to meet the radius of the circle, it seems that Fig.

11 is similar to Fig. 9. However, $a_{n_{cmd}}$ in Table 4 is close to the centripetal acceleration a_{cen}, compared with the results of Table 3. The verification result is shown in Fig. 12.
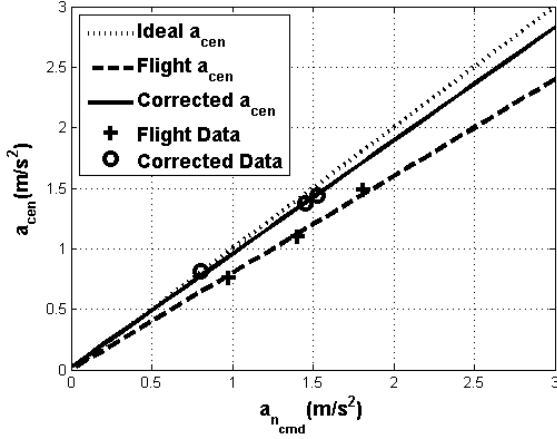

Fig. 12 Modification Result of Flight Test

By applying the modification function $g(\cdot)$, the generated guidance command makes the UAV fly accurately. Before modification, there exists 19.9% acceleration mismatch as shown in Eq. (14). After modification, there exists 6.4% of acceleration mismatch as shown in Eq. (16).

4.2 Leader-Follower Formation Flight

The leader-follower formation flight is also performed using the modified nonlinear guidance. Longitudinal guidance of the leader UAV is to maintain constant cruise airspeed at pre-defined altitude. Longitudinal guidance of the follower UAV is to maintain the pre-defined distance between the leader and follower UAVs by using airspeed command at same altitude.

$$V_{cmd} = V_{cruise} + k_p(d - 30)$$
$$where \ d = \sqrt{(\Delta x)^2 + (\Delta y)^2} \tag{17}$$

Lateral guidance of two UAVs make UAVs fly in pre-defined same square path. The information of state variables of each UAV is shared by FCC telemetry at 10Hz.

Figure 13 shows the result of formation flight test. In this flight, the follower UAV is ordered to fly at 30 meters behind the leader UAV. Leader and follower UAVs follow the square path successively at same altitude. Euler angles of UAV's are shown in Fig. 14, and position, airspeed and distance are shown in Fig.15.
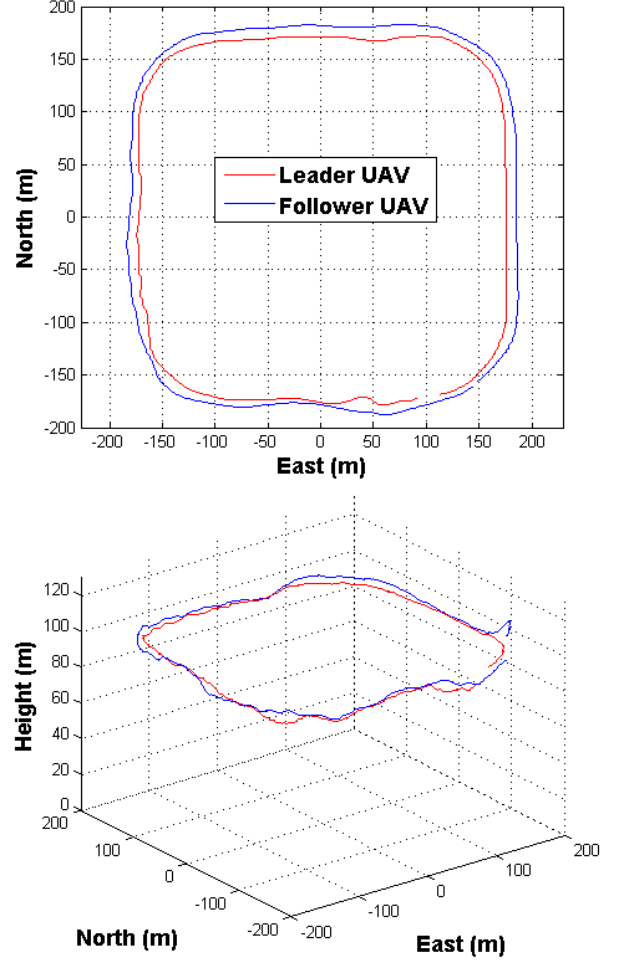

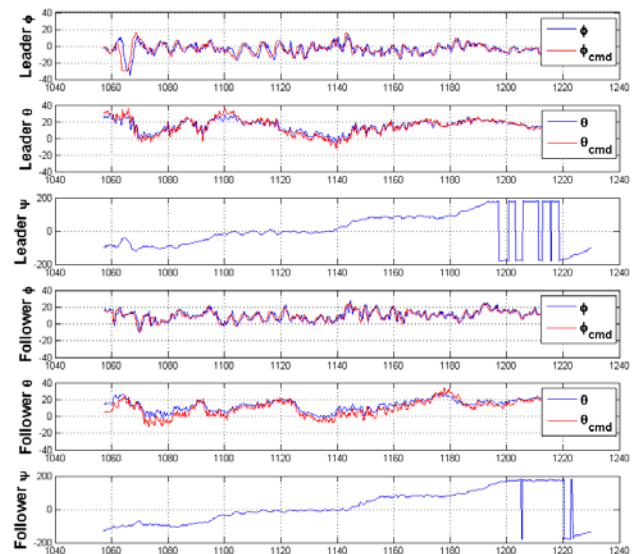**Fig. 13** Leader-Follower Formation Flight 2D and 3D Result

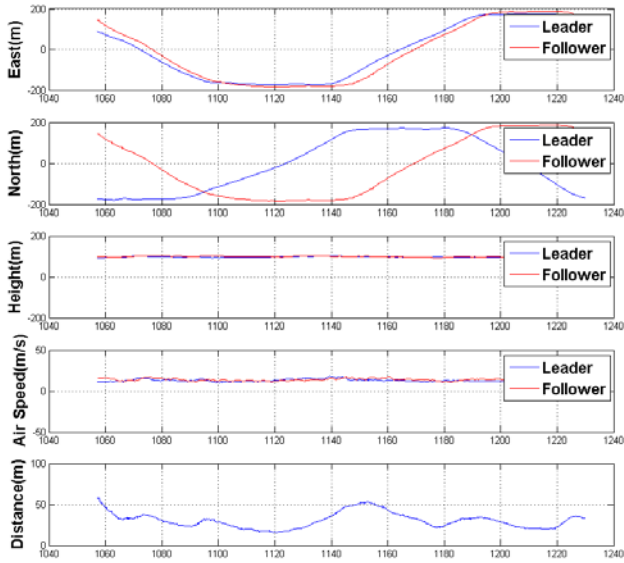**Fig. 14** Leader and Follower Euler Angles

Fig. 15 Leader and Follower Status

5 Conclusion

This paper analyzed the acceleration difference between the geometrically ideal fixed-wing UAV and actual UAV. 6-DOF simulation and flight test result showed that there exists a mismatch between them. The modified guidance law was proposed to compensate the error, and the performance of the proposed scheme was proved by actual flight test. The modification is based-on simple first order function estimation. Without the proposed modification, guidance performance may be degraded especially for high aspect ratio UAV or rudderless airplane. Precise path following flight test will be conducted as a further study.

References

[1] S. Park, J. Deyst, and J. P. How, "Performance and Lyapunov Stability of a Nonlinear Path-Following Guidance Method," *Journal of Guidance, Control, and Dynamics*, vol. 30, no. 6, pp. 1718-1728, November-December 2007.

[2] G. Campa, B. Seanor, Y. Gu, and M. R. Napolitano, "NLDI Guidance Control Laws for Close Formation Flight," *American Control Conference*, Portland, WA, USA, June 2005.

[3] S. Bayraktar, G. E. Fainekos, and G. J. Pappas, "Experimental Cooperative Control of Fixed-Wing Unmanned Aerial Vehicles," *Conference on Decision and Control*, Atlantis, Bahamas, December 2004.

[4] I. Maza, K. Kondak, M. Bernard, and A. Ollero, "Multi-UAV Cooperation and Control for Load Transportation and Deployment," *Journal of Intelligent and Robotic Systems*, vol. 57, Issues 1-4, pp. 417-449, January 2010.

[5] G. Oh, C. Park, M. Kim, J. Park, and Y. Kim, "Small UAV System Identification in Time Domain," *Spring Conference of KSAS*, High One Resort, Gangwon-do, Korea, April 2012.

[6] D. Kim, S. Park, S. Nam, and J. Suk, "A Modified Nonlinear Guidance Logic for a Leader-Follower Formation Flight of Two UAVs," *International Conference on Control, Automation Systems-SICE*, Fukuoka, Japan, August 2009.

[7] Z. Mahboubi, Z. Kolter, T. Wang, and G. Bower, "Camera Based Localization for Autonomous UAV Formation Flight," *Infortech*, St. Louis, MI, USA, March 2011.

[8] A. Verma, C. Wu, and V. Castelli, "UAV Formation Command and Control Management," *2nd AIAA Unmanned Unlimited System, Technologies, and Operations*, San Diego, CA, USA, September 2003.

Contact Author Email Address

- Chulwoo Park (mailto:bakgk@snu.com)
- Hyoun Jin Kim (mailto: hjinkim@snu.ac.kr)
- Youdan Kim (corresponding author, mailto: ydkim@snu.ac.kr)

Acknowledgments

Copyright Statement